

## Design of blade-shaped-electrode linear ion traps with reduced anharmonic contributions

K. Deng, H. Che, Y. Lan, Y. P. Ge, Z. T. Xu, W. H. Yuan, J. Zhang, and Z. H. Lu

Citation: [Journal of Applied Physics](#) **118**, 113106 (2015); doi: 10.1063/1.4931420

View online: <https://doi.org/10.1063/1.4931420>

View Table of Contents: <http://aip.scitation.org/toc/jap/118/11>

Published by the [American Institute of Physics](#)

---

### Articles you may be interested in

[Minimization of ion micromotion in a Paul trap](#)

[Journal of Applied Physics](#) **83**, 5025 (1998); 10.1063/1.367318

[Precise determination of micromotion for trapped-ion optical clocks](#)

[Journal of Applied Physics](#) **118**, 104501 (2015); 10.1063/1.4930037

[A modified model of helical resonator with predictable loaded resonant frequency and Q-factor](#)

[Review of Scientific Instruments](#) **85**, 104706 (2014); 10.1063/1.4897478

[Operating Parameters of a Quadrupole in a Grounded Cylindrical Housing](#)

[Journal of Vacuum Science and Technology](#) **8**, 266 (1971); 10.1116/1.1316304

[Cryogenic setup for trapped ion quantum computing](#)

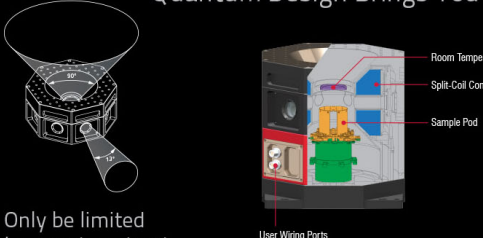
[Review of Scientific Instruments](#) **87**, 113103 (2016); 10.1063/1.4966970

[An integrated mirror and surface ion trap with a tunable trap location](#)

[Applied Physics Letters](#) **109**, 221108 (2016); 10.1063/1.4970542

---

Quantum Design Brings You the Next Generation Magneto-Optic Cryostat




Only be limited by your imagination...

Room Temperature Window  
Split-Coil Conical Magnet  
Sample Pod  
User Wiring Ports

[Learn More](#)

Quantum Design  
qdusa.com/opticool5

8 Optical Access Ports: 7 Side; 1 Top  
Temperature Range: 1.7 K to 350 K  
7 T Split-Coil Conical Magnet  
Low Vibration: <10 nm peak-to-peak  
89 mm x 84 mm Sample Volume  
Automated Temperature & Magnet Control  
Cryogen Free



# Design of blade-shaped-electrode linear ion traps with reduced anharmonic contributions

K. Deng,<sup>1</sup> H. Che,<sup>1</sup> Y. Lan,<sup>1,2</sup> Y. P. Ge,<sup>1</sup> Z. T. Xu,<sup>1</sup> W. H. Yuan,<sup>1</sup> J. Zhang,<sup>1</sup> and Z. H. Lu<sup>1,a)</sup>

<sup>1</sup>MOE Key Laboratory of Fundamental Physical Quantities Measurement, School of Physics, Huazhong University of Science and Technology, 1037 Luoyu Road, Wuhan 430074, People's Republic of China

<sup>2</sup>Department of Physics and Astronomy, University of British Columbia, Vancouver, BC V6T 1Z1, Canada

(Received 15 July 2015; accepted 8 September 2015; published online 18 September 2015)

RF quadrupole linear Paul traps are versatile tools in quantum physics experiments. Linear Paul traps with blade-shaped electrodes have the advantages of larger solid angles for fluorescence collection. But with these kinds of traps, the existence of higher-order anharmonic terms of the trap potentials can cause large heating rate for the trapped ions. In this paper, we theoretically investigate the dependence of higher-order terms of trap potentials on the geometry of blade-shaped traps, and offer an optimized design. A modified blade electrodes trap is proposed to further reduce higher-order anharmonic terms while still retaining large fluorescence collection angle. © 2015 AIP Publishing LLC. [<http://dx.doi.org/10.1063/1.4931420>]

## I. INTRODUCTION

Laser-cooled ions trapped in linear Paul traps can be treated as ideal quantum systems that are free from environmental perturbations. In recent years, ion traps have become powerful tools in experimental investigation of quantum information processing,<sup>1,2</sup> high precision spectroscopy,<sup>3–5</sup> and cavity quantum electrodynamics.<sup>6</sup> The traps are often designed to have enough space for laser cooling, ions state manipulation, and read out.

Using linear Paul traps to control charged particles was first proposed by Prestage *et al.*<sup>7</sup> In an ideal linear Paul trap, the surface of electrodes has hyperbolic shape, and a pure quadrupole electric potential is produced in the radial direction if we neglect the effects of DC electrodes. Under this potential, ion motion is governed by the Mathieu equation. The solution of the Mathieu equation describes ions' motions inside a trap. The motional spectrum contains frequencies of secular motion and micromotion.<sup>8</sup>

For a realistic linear Paul trap, the electrodes cannot be infinitely large to meet the boundary condition of a pure quadrupole potential (the equipotential shape). Electrodes have to be truncated at an acceptable length. In addition, in an ideal linear Paul trap, the electrodes fill up almost all the transverse plane, restricting laser beams' access as well as fluorescence collection access. In order to meet the larger opening requirement for laser cooling and fluorescence collection, the hyperbolic electrodes are replaced with circular shape electrodes, and these electrodes can be truncated at a smaller extension.<sup>9</sup>

In order to provide the required electric potential strength to confine ions with reasonable voltages on the electrodes, the radial distance of the electrodes should be as close as possible. However, when the radial distance of the trap is reduced, it is difficult to properly hold the electrodes during fabrication process, especially when relatively high

assembling precision is required. In addition, when we reduce the radial distance of the trap, the trap is not stable enough with applied high RF voltages. To avoid these problems, blade-shaped electrodes are introduced so that relatively high precision at these small scales could be reached. Blade-shaped electrodes were first used at Innsbruck.<sup>10</sup> Electrostatic simulation of this structure was done to calculate the axial and radial frequency of ions' motion in the trap. In the calculation, the electric potential quadratic term was calculated, but higher-order electric potential terms were not discussed. Since the blade-shaped electrodes may deviate more from the perfect hyperboloid shape, their electric potential will have more higher-order terms contribution. To our knowledge, numerous papers have discussed circular<sup>11–13</sup> and hyperbolic<sup>14,15</sup> electrodes' anharmonic potential terms, but there is no detailed analysis of blade-shaped electrodes anharmonic potential terms.

These anharmonic potentials act on the trapped ions, and give rise to fluctuating forces on the ions. This will heat the ions. The heating rate is used to describe the heating effect, which equals to the average number of quanta of energy gained by the ion secular motion in a given time. For a particle of charge  $q$  and mass  $m$  trapped in a harmonic potential, the heating rate is generalized to be<sup>16</sup>

$$\frac{dn}{dt} = \frac{q^2}{4m\hbar\omega_m} \left[ S_E(\omega_m) + \frac{\omega_m^2}{2\Omega^2} S_E(\Omega \pm \omega_m) \right], \quad (1)$$

where  $\omega_m$  is the secular motion frequency of the motion mode under consideration,  $S_E$  is the spectral density of electric-field fluctuations in units of  $(V/cm)^2 Hz^{-1}$ , and  $\Omega$  is the RF drive frequency of the trap.

Large heating rate has many negative effects. It can drive ions out of an initially prepared motional ground state,<sup>17</sup> and also can lead to decoherence of the quantum superposition states.<sup>18</sup> Additionally, it will potentially limit the achievable temperature of laser cooling, prevent the formation of ion crystals, and limit the trapping lifetime of ions and length of

<sup>a)</sup>Electronic address: zehuangu@mail.hust.edu.cn

quantum logic gate operations, as well as requiring more elaborate cooling and error correction schemes. Therefore, reducing the anharmonic potentials to acceptable values presents a great challenge in ion trap design.

In this work, we calculate the anharmonic trapping potential terms of blade-shaped electrodes linear Paul traps. Influence of geometry dimension of blade-shaped electrodes on the anharmonic potential terms is theoretically studied. Fluorescence collection efficiency is also considered in the trap design. Based on the calculation results, an optimized trap design is given. The results demonstrate a blade-shaped electrodes linear Paul trap with low anharmonic terms and favorable fluorescence collection angle. In addition, we propose a novel design of blade to further reduce the anharmonic terms while keeping the large fluorescence collection angle.

## II. TRAP DESIGN

The initial design of Paul trap uses hyperbolic quadrupole electrodes.<sup>19</sup> Inside the trap where no charge exists, electrical potential distribution obeys the Laplace equation  $\nabla^2\Phi=0$ . Therefore, the potential is determined by the voltages on the electrodes surfaces which function as boundary conditions for the potential distribution. If the inner zone of trap is not well shielded by the electrodes, the external environment can also affect the potential distribution. However, this is usually not considered as a problem due to its small effect. Assuming the electrodes are long enough, electrical

potential at the transverse plane near the trap center would be uniform.

In order to realize larger opening for laser cooling and fluorescence collection, in many applications, the hyperbolic electrodes are replaced with circular shape electrodes, which are easier to fabricate and mount with high precision. The potential distribution of circular electrodes in the transverse plane near the trap center can be expressed as an infinite series<sup>11</sup>

$$\Phi(r, \theta) = (U_0 + V_0 \cos \omega t) \sum_n C_n \left(\frac{r}{r_0}\right)^n \cos n\theta, \quad (2)$$

where  $U_0$  is the applied DC voltage,  $V_0$  is the peak voltage of the applied RF drive,  $r_0$  is the distance from the center of the trap to the electrodes. When distortions of the quadrupole potential at the traps' center plane are discussed, the potential is usually given by the multipole expansion of the potential  $\Phi(x, y)$ :<sup>12</sup>

$$\Phi(x, y) = \sum_{n=0} \frac{K_n \phi_n}{r_0^n} = A_0 + \sum_{n=2} A_n \phi_n, \quad (3)$$

where  $K_n$  is the amplitude of a multipole  $\phi_n$  with  $2n$  poles. With the exception of the first term, the symmetry of electrodes' geometry and boundary conditions requires that only  $n=2(2m+1)$  ( $m=0, 1, 2, \dots$ ) terms exist. The first few terms of  $\Phi(x, y)$  are

$$\begin{aligned} \Phi_0 &= A_0, \\ \Phi_2 &= A_2(x^2 - y^2), \\ \Phi_6 &= A_6(x^6 - 15x^4y^2 + 15x^2y^4 - y^6), \\ \Phi_{10} &= A_{10}(x^{10} - 45x^8y^2 + 210x^6y^4 - 210x^4y^6 + 45x^2y^8 - y^{10}), \\ \Phi_{14} &= A_{14}(x^{14} - 91x^{12}y^2 + 1001x^{10}y^4 - 3003x^8y^6 + 3003x^6y^8 - 1001x^4y^{10} + 91x^2y^{12} - y^{14}). \end{aligned}$$

Here, the first term is quadrupole offset potential. The second term is the quadrupole term, which is called  $A_2$  term since it corresponds to  $n=2$ . The third term is called  $A_6$  term which corresponds to  $n=6$ , and it is the second largest potential terms in the central trap region. In order to obtain the best approximation to a pure quadrupole potential, the  $A_6$  term should be minimized in the trap design. It has been found that for circular electrodes, the  $A_6$  term vanishes when  $r_e/r_0 = \eta = 1.14511$ ,<sup>20</sup> where  $r_e$  is the radius of the circular electrodes. Definition of  $r_0$  and  $r_e$  for the circular electrodes trap is shown in Fig. 1(a).

The circular electrodes' distance to trap center  $r_0$  greatly affects the trap's required RF drive power. If we only consider regular RF power that can be realized in a typical experimental setup, a reasonable value of  $r_0$  would be less than 1 mm. Under this situation, it is difficult to hold the electrodes in the fabrication process, especially when a relatively high precision assembling is required. In our case, the precision should be about 20  $\mu\text{m}$ . Trap metal electrodes fabricated

using the wire electrical discharging machining can reach a precision of 10  $\mu\text{m}$ . The trap holders machined using the computer numerical controlled milling machine can reach precision of 10–20  $\mu\text{m}$ . In previous experiments, we assembled a trap with 200  $\mu\text{m}$  displacement. In that case, the micromotion is very hard to compensate since the needed compensation voltage is more than 2500 V. For another trap with 70  $\mu\text{m}$  displacement, the compensation voltage is decreased to 1200 V.

A blade-shaped electrodes' construction with high precision at these small scales is a good solution for trap fabrication. The basic idea is to connect each rod electrode with a blade together, and the blade has relatively large area and is easy to be supported on the trap holder. In practice, blade-shaped electrodes are designed to be an oblique body with rounded edge. The farther part of the blade is used for supporting the critical edge, and to be mounted in the trap holder.

Just like in the design of circular electrodes linear Paul traps, in the design of blade-shaped electrodes linear traps, it

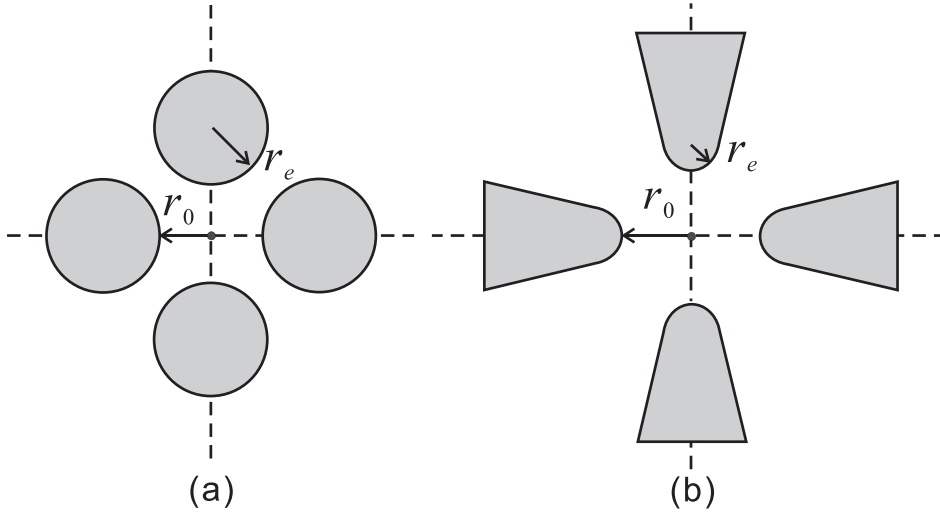


FIG. 1. Definition of  $r_0$  and  $r_e$  in cross section of circular electrodes trap (a) and blade electrodes trap (b).

is necessary to consider two parameters, distance of the blades' inner surface to the trap center  $r_0$ , and the radius of curvature of the blades  $r_e$ . Definition of  $r_0$  and  $r_e$  for the blade-shaped electrodes linear traps is shown in Fig. 1(b). In the following part, the two parameters are set as variable parameters to find a configuration with the smallest anharmonic potential terms.

First, we considered the effect of the distance of the two opposite blades  $2r_0$ . If  $r_0$  is too large, the secular frequency would be low since

$$\omega_{r_0} \propto \frac{qV_0}{m\Omega r_0^2}. \quad (4)$$

However, in many experiments, higher secular frequency is preferred so that strong binding limit and smaller Lamb-Dicke parameter are easier to be achieved. Higher secular frequency will also facilitate faster ions motional ground state cooling. Therefore, a large  $r_0$  is not appropriate. On the other hand, down-sizing the trap will cause serious heating problems according to earlier experiments.<sup>16</sup> We choose  $r_0$

to be a moderate value of 0.8 mm, and then we will try to find the best  $r_e$  for the ion traps.

Since  $A_2$  term is the needed quadrupole term to drive and confine ions, we are interested in ratio of  $A_6$ ,  $A_{10}$ ,  $A_{14}$  to  $A_2$ . Since they have different units, we choose to compare their normalized counterparts, namely,  $K_2$ ,  $K_6$ ,  $K_{10}$ ,  $K_{14}$ . The relationship between them is  $A_n = K_n/r_0^n$ , where the normalization factor  $r_0$  is chosen to be 0.8 mm. Apparently with this normalization, all  $K_n$  terms have the same unit.

We used the Computer Simulation Technology (CST) software to calculate electrical potential distribution of the trap with a  $r_e$ . Then we least-squares fit the ratios of  $K_6$ ,  $K_{10}$ ,  $K_{14}$  to  $K_2$ . Then the simulation was repeated under different  $r_e$ . These values as a function of rounding diameter  $2r_e$  are plotted in Fig. 2. It can be seen that when the rounding diameter is less than 1.8 mm, larger rounding diameter produces smaller higher order potential terms. However, larger rounding diameter may block the path for fluorescence collection. Figure 3 shows the fluorescence collection solid angle as a function of rounding diameter. At 1.8 mm, the fluorescence collection solid angle is only 0.16 Sr. Since in most trap

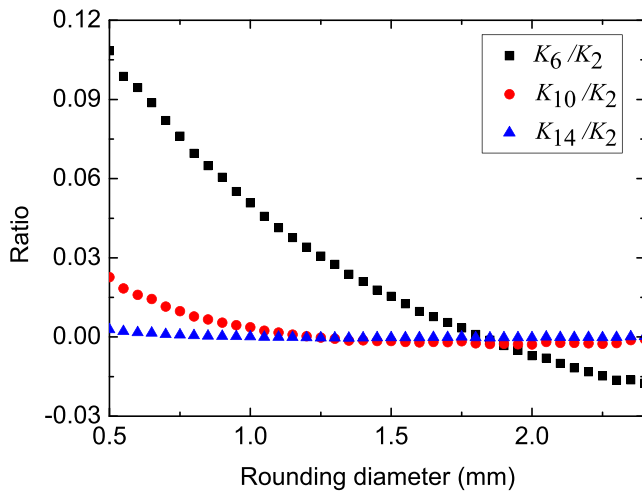


FIG. 2. Ratio of anharmonic terms  $K_6$ ,  $K_{10}$ ,  $K_{14}$  to  $K_2$  as a function of rounding diameter  $2r_e$  for the blade electrodes trap.  $K_n$  is defined in Eq. (3). In the simulation,  $r_0$  is set to 0.8 mm.

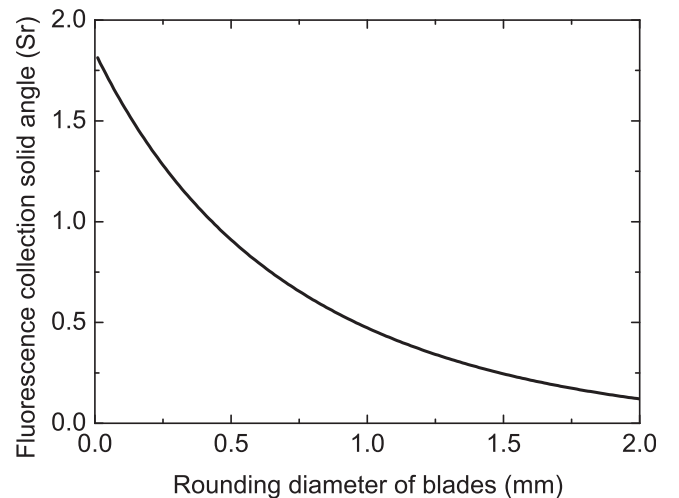


FIG. 3. Fluorescence collection solid angle of blade electrodes traps as a function of rounding diameter  $2r_e$ .

applications a larger fluorescence collection solid angle is preferred, a smaller rounding diameter is required. To balance these two requirements, radius of the electrodes edge is chosen to be  $r_e = 0.3$  mm. This design enables a rather large fluorescence collection solid angle of about 0.80 Sr, which is four times more than that of circular electrodes at its optimum design of  $r_e/r_0 = \eta = 1.14511$ . Based on a trap in our lab with the collection solid angle of about 0.80 Sr, a count rate of about 250 kHz is observed from a single  $^{25}\text{Mg}^+$  ion at saturation intensity, and a signal to noise ratio of 100 is reached. In this case, the corresponding anharmonic electrical potential terms are still reasonably small ( $K_6/K_2 = 0.1$ ).

### III. A NOVEL DESIGN OF BLADE ELECTRODES

If the higher order anharmonic terms need to be further reduced while keeping the trap's fluorescence collection solid angle, a geometry compensation method for blade-shaped electrodes can be implemented. To explain the mechanism of this compensation method, equipotential contours for hyperbolic electrodes, blade-like electrodes, circular electrodes, and the novel electrodes are shown in Fig. 4. The equipotential contours of pure quadrupole term are plotted as the white dashed lines. In Fig. 4(a), it can be seen that for the hyperbolic electrodes, the equipotential contours of quadrupole term well match the equipotential lines of real electrodes. For circular electrodes in Fig. 4(b), the ratio  $r_e/r_0 = \eta = 1.14511$ , so in the center region, the equipotential contours still match quadrupole lines well, but they deviate

from quadrupole lines when they are far from the trap center (close to electrodes). However, for this trap geometry, the fluorescence collection angle is not favorable. For the blade-shaped electrodes in Fig. 4(c), the ratio  $r_e/r_0$  is 0.37, which gives a large collection solid angle of 0.80 Sr. The deviation of equipotential contours from quadrupole lines is more serious. Cause of this deviation is obvious from the comparison between Figs. 4(b) and 4(c). The blade-shaped electrodes are too sharp. For each fixed voltage, the real equipotential exceeds the quadrupole's at the radial direction. Based on above observation, we propose a geometry compensation method to refine the non-hyperbolic quadrupole traps. Inspiration of this method comes from harmonic tuning of ancient eastern musical instruments *Xiao* and *Shakuhachi*. A cutting in the electrodes' front draws back the equipotential lines radially as a compensation. The modified electrodes together with the equipotential contour are shown in Fig. 4(d) for these modified-blade electrodes. Compared with Fig. 4(c), it can be seen that the real equipotential agrees quadrupole potential very well in the area near the trap center even though the potential near electrodes deviates seriously.

In order to tune the electrodes' potential terms, the geometry of the blade should be carefully designed. We defined two characteristic parameters for modified-blade electrodes. They are cutting and filleting, as shown in Fig. 5. Simulation results show that the  $A_6$  term can be made zero by changing the characteristic parameters. In simulation, the cutting is chosen from 0.2 mm to 1.5 mm. Note that the

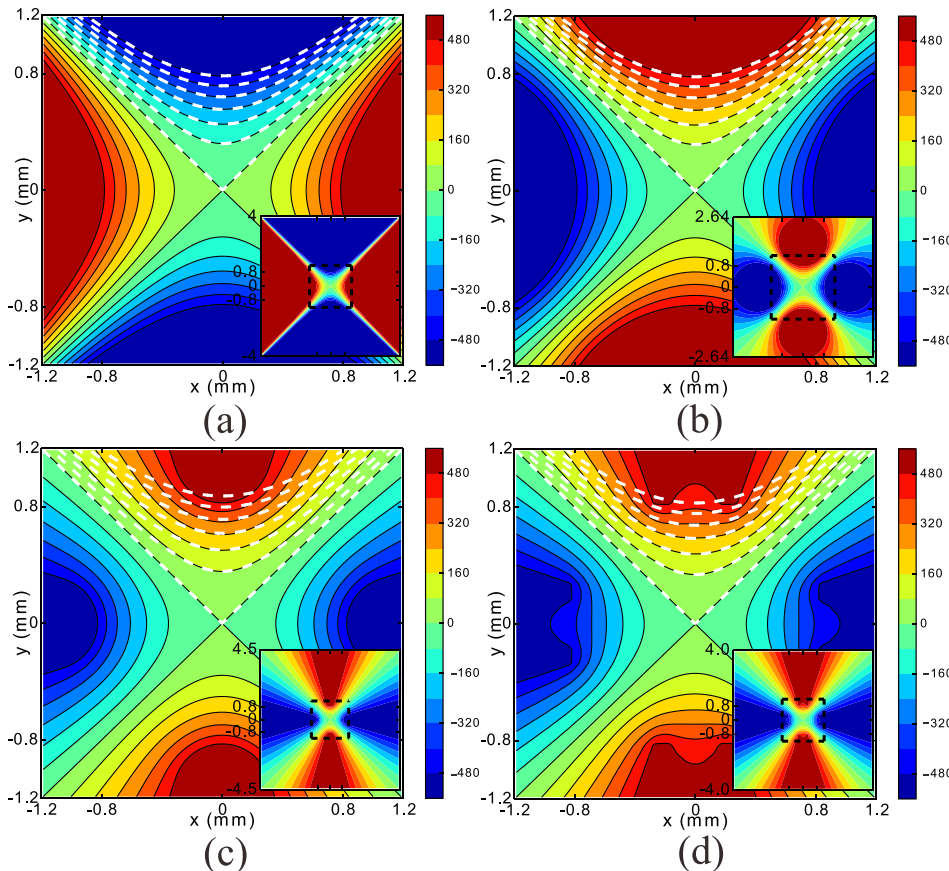


FIG. 4. The equipotential contours for (a) hyperbolic electrodes, (b) circular electrodes, (c) blade electrodes, and (d) blade-modified electrodes. The equipotential contours of pure quadrupole are plotted as the white dashed lines. For (a) and (b), the equipotential contour matches the quadrupole lines well but the fluorescence collection angle is very small. For (c), the real equipotential exceeds the quadrupole's at the direction of blade to electrodes center. For (d), the equipotential contour matches the quadrupole potential lines very well again in the region near the trap center. Insets show fuller view of the potential distribution.



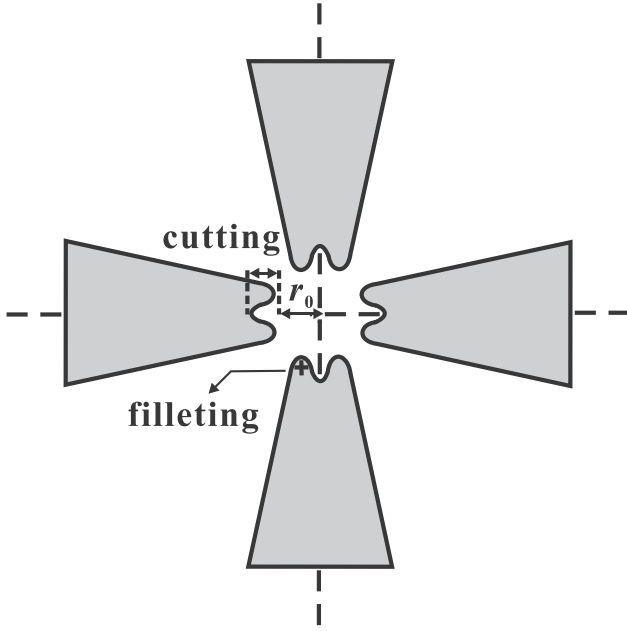
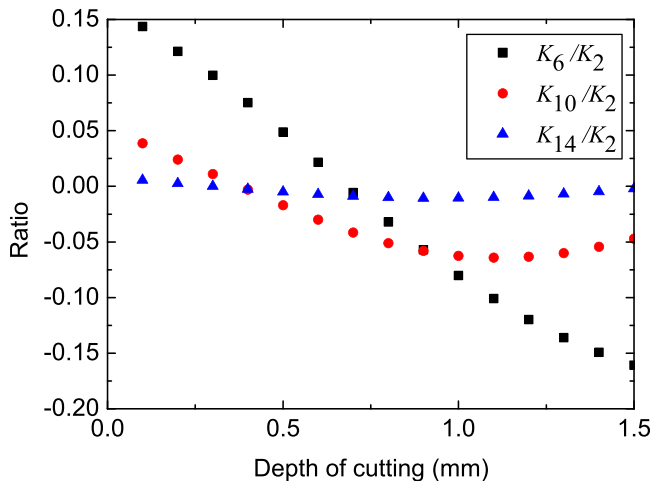


FIG. 5. Cross section of the modified-blade electrodes.

bottom of the cutting should not be too sharp, or it may affect the vacuum pumping ability. Some typical results are shown in Fig. 6. In Fig. 6,  $r_0$  is chosen to be 0.8 mm, this is the same as discussed before in Section II, and filleting is 0.1 mm. The figure shows that the ratio of anharmonic terms  $K_6$ ,  $K_{10}$ ,  $K_{14}$  to  $K_2$  as a function of cutting depth. It can be seen that when the cutting depth is adjusted appropriately, we can tune the  $A_6$  term to be zero, which is the most important operating parameter for ion traps. In comparison with blade-electrodes trap design and modified-blade electrodes trap design, under the same fluorescence collection angle, the modified-blade electrodes  $A_6$  terms will be much smaller, and consequently contributing less to the heating rate.

In real applications, due to machining tolerance, there is uncertainty for the amount of filleting. In Fig. 6, where the filleting is 0.1 mm, if the machining uncertainty is  $10\ \mu\text{m}$ , the calculated ratio of  $K_6/K_2$  has an uncertainty of 0.001. For

FIG. 6. Ratio of anharmonic terms  $K_6$ ,  $K_{10}$ ,  $K_{14}$  to  $K_2$  as a function of depth of cutting for the modified-blade electrodes traps.

comparison, the ratio of  $K_6/K_2$  has an uncertainty of 0.002 if the cutting uncertainty is also  $10\ \mu\text{m}$ . From our experience, a machining tolerance of  $20\ \mu\text{m}$  is acceptable.

#### IV. CONCLUSION

In conclusion, we study the effect of trap geometry on anharmonic potential terms for blade-shaped electrodes linear Paul traps. The simulation results show how the trap design can be optimized to reduce anharmonic terms while meeting requirement of large fluorescence collection angle. Furthermore, a modified blade model is proposed to null the  $A_6$  term while keeping a large fluorescence collection solid angle. The study will be useful in ion-trap-related precision measurement experiments.

#### ACKNOWLEDGMENTS

The project is partially supported by the National Basic Research Program of China (Grant No. 2012CB821300), the National Natural Science Foundation of China (Grant Nos. 11304109, 11174095, and 91336213), and Program for New Century Excellent Talents by the Ministry of Education.

- <sup>1</sup>H. Haffner, W. Hansel, C. F. Roos, J. Benhelm, D. C. Alkar, M. Chwalla, T. Korber, U. D. Rapol, M. Riebe, P. O. Schmidt, C. Becher, O. Guhne, W. Dur, and R. Blatt, "Scalable multiparticle entanglement of trapped ions," *Nature* **438**, 643 (2005).
- <sup>2</sup>D. B. Hume, T. Rosenband, and D. J. Wineland, "High-fidelity adaptive qubit detection through repetitive quantum nondemolition measurements," *Phys. Rev. Lett.* **99**, 120502 (2007).
- <sup>3</sup>T. Rosenband, D. B. Hume, P. O. Schmidt, C. W. Chou, A. Brusch, L. Lorini, W. H. Oskay, R. E. Drullinger, T. M. Fortier, J. E. Stalnaker, S. A. Diddams, W. C. Swann, N. R. Newbury, W. M. Itano, D. J. Wineland, and J. C. Bergquist, "Frequency ratio of  $\text{Al}^+$  and  $\text{Hg}^+$  single-ion optical clocks; metrology at the 17th decimal place," *Science* **319**, 1808 (2008).
- <sup>4</sup>J. C. J. Koelmeij, B. Roth, A. Wicht, I. Ernsting, and S. Schiller, "Vibrational spectroscopy of  $\text{HD}^+$  with 2-ppb accuracy," *Phys. Rev. Lett.* **98**, 173002 (2007).
- <sup>5</sup>Y. Wan, F. Gebert, F. Wolf, and P. O. Schmidt, "Efficient sympathetic motional-ground-state cooling of a molecular ion," *Phys. Rev. A* **91**, 043425 (2015).
- <sup>6</sup>P. F. Herskind, A. Dantan, J. P. Marler, M. Albert, and M. Drewsen, "Realization of collective strong coupling with ion Coulomb crystals in an optical cavity," *Nat. Phys.* **5**, 494 (2009).
- <sup>7</sup>J. D. Prestage, G. J. Dick, and L. Maleki, "New ion trap for frequency standard applications," *J. Appl. Phys.* **66**, 1013 (1989).
- <sup>8</sup>D. J. Berkeland, J. D. Miller, J. C. Bergquist, W. M. Itano, and D. J. Wineland, "Minimization of ion micromotion in a Paul trap," *J. Appl. Phys.* **83**, 5025 (1998).
- <sup>9</sup>M. E. Poitzsch, J. C. Bergquist, W. M. Itano, and D. J. Wineland, "Cryogenic linear ion trap for accurate spectroscopy," *Rev. Sci. Instrum.* **67**, 129 (1996).
- <sup>10</sup>F. Schmidt-Kaler, H. Haffner, S. Gulde, M. Riebe, G. P. T. Lancaster, T. Deuschle, C. Becher, W. Hansel, J. Eschner, C. F. Roos, and R. Blatt, "How to realize a universal quantum gate with trapped ions," *Appl. Phys. B* **77**, 789 (2003).
- <sup>11</sup>D. R. Denison, "Operating parameters of a quadrupole in a grounded cylindrical housing," *J. Vac. Sci. Technol.* **8**, 266 (1971).
- <sup>12</sup>D. J. Douglas and N. V. Kononov, "Influence of the 6th and 10th spatial harmonics on the peak shape of a quadrupole mass filter with round rods," *Rapid Commun. Mass Spectrom.* **16**, 1425 (2002).
- <sup>13</sup>J. Pedregosa, C. Champenois, M. Houssin, and M. Knoop, "Anharmonic contributions in real RF linear quadrupole traps," *Int. J. Mass Spectrom.* **290**, 100 (2010).
- <sup>14</sup>R. Alheit, C. Hennig, R. Morgenstern, F. Vedel, and G. Werth, "Observation of instabilities in a Paul trap with higher-order anharmonicities," *Appl. Phys. B* **61**, 277 (1995).

- <sup>15</sup>T. Gudjons, P. Seibert, and G. Werth, "Influence of anharmonicities of a Paul trap potential on the motion of stored ions," *Appl. Phys. B* **65**, 57 (1997).
- <sup>16</sup>Q. A. Turchette, D. Kielpinski, B. E. King, D. Leibfried, D. M. Meekhof, C. J. Myatt, M. A. Rowe, C. A. Sackett, C. S. Wood, W. M. Itano, C. Monroe, and D. J. Wineland, "Heating of trapped ions from the quantum ground state," *Phys. Rev. A* **61**, 063418 (2000).
- <sup>17</sup>D. F. V. James, "Theory of heating of the quantum ground state of trapped ions," *Phys. Rev. Lett.* **81**, 317 (1998).
- <sup>18</sup>C. J. Myatt, B. E. King, Q. A. Turchette, C. A. Sackett, D. Kielpinski, W. M. Itano, C. Monroe, and D. J. Wineland, "Decoherence of quantum superpositions through coupling to engineered reservoirs," *Nature* **403**, 269 (2000).
- <sup>19</sup>P. Wolfgang, "Electromagnetic traps for charged and neutral particles," *Rev. Mod. Phys.* **62**, 531 (1990).
- <sup>20</sup>A. J. Reuben, G. B. Smith, P. Moses, A. V. Vagov, M. D. Woods, D. B. Gordon, and R. W. Mund, "Ion trajectories in exactly determined quadrupole fields," *Int. J. Mass Spectrom. Ion Phys.* **154**, 43 (1996).